The Young Local Associations as seen by Gaia

Author: Núria Miret Roig
Facultat de Física, Universitat de Barcelona, Diagonal 645, 08028 Barcelona, Spain.

Advisor: Mercè Romero-Gómez

Abstract: The aim of this project is to study the capabilities of the current and near future Gaia astrometric and spectroscopic surveys to derive the dynamical age and place of birth of the Young Local Associations (YLAs). We find that already with the accuracies of the Gaia DR1 we are able to study membership and the signatures of the potential. Furthermore, with DR1 we can do a first attempt to determine the place of birth of the association. This will be improved with Gaia end-of-mission accuracies when we will also be able to determine the dynamical ages.

I. INTRODUCTION

The Young Local Associations (YLAs) are defined as groups of stars of ages between $8 - 50$ Myr, at less than 100 pc from the Sun, with relatively low densities compared to the field, which share common motions and are chemically homogeneous. As excellent tracers of the young population in the solar neighbourhood, they allow us to study the mechanisms driving the star formation process and secular evolution of the Milky Way (MW) thin disc population. Several YLA have been defined thanks to the first Hipparcos astrometry (e.g. [17], [7], [25]). Nonetheless, their discovery and membership evaluation is highly demanding in terms of both, the observational data required (accurate astrometry and spectroscopy) and the kinematical and dynamical analysis. The 6D phase space (positions and velocities) shall be combined with realistic Galactic potentials to integrate their orbits back in time to characterize this population at birth. Undoubtedly, Gaia data combined with accurate spectroscopy will provide critical new insights in this study.

Fernández et al. [7] published a first compilation of data regarding the YLAs after Hipparcos (see Table 1 in their paper). For 8 different YLAs, they provide the mean spatial and kinematic properties, ages (between 5 and 30-150 Myr) and number of members (ranging form 5 to 59). They found large uncertanties in the ages published in the literature. The errors in Hipparcos positions and parallaxes were of 1 mas in mean and in proper motions of 1 mas yr^{-1} in mean [24]. Fernández et al. [7] assumed unrealistic errors in radial velocity (RV) of less than 2 km s^{-1} for most of the stars. The large errors in astrometry did not allow them clearly to confirm their hypothesis of YLAs being formed due to the impact of the inner spiral arm shock wave against a giant molecular cloud. More recently, a lot of effort has been devoted to search for new members to the already known YLAs. For instance, Binks et al. [5] use superWASP spectroscopy to obtain rotation periods, ROSAT X-ray emission and NOT spectra to derive Lithium equivalent widths (LiEW), Hα emission, projected rotational velocities ($v \sin i$) and RV to search new candidates to nearby young associations. Elliott et al. [18] also update and search for new members to the young associations in the original Search for Associations Containing Young stars (SACY) [17]. Here the authors combine 2MASS photometry and proper motions from UCAC4, PPMXL and NOMAD. Nowadays, several groups have developed probabilistic methods to assess membership for candidates to belong to the YLAs. For instance, Klutsch et al. [11] present two independent procedures based on the kinematic analysis plus other indicators such as chromospheric activity, age proxies (lithium abundance), and chemical composition. Riedel et al. [19] present a program in python LACEwING (LocAting Constituent mEmbers In Nearby Groups) which uses the kinematics (positions and motions) of stars to determine if they are members of one of 10 nearby (within 100 parsecs) young moving groups or 4 nearby open clusters. Malo et al. [13] and Gagné et al. [6] present a Bayesian Analysis for Nearby Young Associations (BANYAN I and II). The analysis takes into account the position, proper motion, magnitude, and colour of the star, but other observables can be readily added (e.g., RV, distance). They use this method to find new young low-mass stars in the β Pictoris and AB Doradus moving groups and in the TW Hydrae, Tucana-Horologium, Columba, Carina, and Argus associations.

In this project we focus on the less studied traceback analysis to perform back-in-time integrations to recover the place of birth and the dynamical age of a given YLA. We want to study both the effects of the non-axisymmetric components of the Galactic potential and the different astrometric and RV accuracies. To do so, we have two strong hypothesis, namely that the Galactic potential is known and that the birth initial conditions of the YLA are known.

II. SETTING THE REQUIREMENTS TO STUDY THE ORIGIN OF THE YLA

In this section we describe the model and the strategy we use to study the origin of the YLAs. We aim to set the requirements necessary for this purpose, that is to say, which parameters in the phase space are essential and the maximum errors acceptable in order to find both

the dynamical age and the birth place of the YLA.

A. The MW Galactic potential

Here we give a short description of the two Galactic potentials used in the integration, namely the bar model and the spiral model.

The bar model consists of the superposition of an axisymmetric component (given by [1]) and two Ferrers bars to model the Galactic bar (COBE/DIRBE bulge plus Long bar), as in [20]. Both are aligned and they are 20° from the Sun-Galactic Centre line, towards positive galactic longitudes. The Galactic bar rotates at a constant pattern speed of 50 km s^{-1}kpc^{-1}. The Galactic bar is introduced adiabatically in 4 bar rotations and its mass is the same as the spherical bulge in [1]. In order to conserve the total mass of the Galaxy, we reduce the mass of the spherical bulge at the same time the Galactic bar is introduced. Therefore, at the final configuration, the bulge mass is transferred to the Galactic bar.

The spiral model consists of the superposition of the same axisymmetric component and the PERLAS arms as in [15], [2]. With this spiral model we pretend to study the effect of a more local perturbation in the integration of the YLAs. The spiral model is also 3D and the spiral has an amplitude of 5% of the disc mass, this is the maximum amplitude determined by the observations [2]. In this case, the spiral arms are totally included in the Galactic potential and they are not introduced adiabatically, as in the bar model. We consider two different cases for this spiral model changing only the pattern speed of the spiral arms, namely 20 km s^{-1}kpc^{-1}, and we refer to it as PERLAS-20, and 30 km s^{-1}kpc^{-1}, PERLAS-30.

B. Integration process, orbits back in time

Here we describe the integration process step by step. First, we define a mother particle (M) at $T = 0$ with an initial position $\mathbf{R}_{M,0}$ and initial velocity $\mathbf{V}_{M,0}$ and we integrate this mother particle back in time a given time T. At this point the particle coordinates are $\mathbf{R}_{M,-T}$ and $\mathbf{V}_{M,-T}$. The following steps are:

1. *At birth*: Generate N particles (P) at the same position with null dispersion $\mathbf{R}_{P,-T} = \mathbf{R}_{M,-T}$ and at the same velocity with an isotropic dispersion $(\sigma_U, \sigma_V, \sigma_W) = (2, 2, 2)$ km s^{-1}. After some tests, we have set the dispersions in velocity isotropic for simplicity.

2. *At present*: Integrate the N particles forwards the same time T.

3. *Errors*: Apply errors for positions, parallax, proper motions and RV.

4. *Back in time*: Integrate the orbits back in time the same time T as were integrated forwards.

The positional coordinates used are the curvilinear heliocentric coordinates as defined in [3]. The velocity coordinates used are (U, V, W) with respect to the Local Standard of Rest (LSR), defined as a point in space that is moving on a perfectly circular orbit around the centre of the galaxy at the Sun's galactocentric distance.

C. Simulating a YLA

After making some tests of the model and the process described above with a fiducial particle located at different initial positions and velocities, we show the results for already a realistic case. Here we consider as the mother particle (M) the mean heliocentric position and velocity of TW Hydra with $(\xi', \eta', \zeta')_{M,0}$ = (-21, -53, 21) pc and $(U, V, W)_{M,0}$ = (-9.7,- 17.1, -4.8) km s^{-1} [7] . We choose an integration time of 50 Myr to evaluate the integration process back-in-time. We have considered four different scenarios, summarized in Table I. *Before Gaia* represents essentially the current available data, based on Hipparcos astrometry and current RV surveys. *DR1 TGAS-Hip* and *DR1-TGAS-Tyc* are the two subsets of TGAS (Tycho-Gaia Astrometric Solution [14]) that will be included in Gaia-DR1 expected for end of summer 2016. Finally, *Gaia+* represents the end-of-mission astrometric data together with complementary accurate RV. We assume that the YLA has N detected members with mean apparent magnitude $\langle V \rangle$ and a dispersion of 1 mag around it, that the mean astrometric accuracy for the Hipparcos members at present is 1 mas and 1 mas yr^{-1}, that DR1 data will allow us to double the number of members (from 20 to 50), that at the end of Gaia mission we will have accurate RV (σ_{RV} = 0.5 km s^{-1}) from the on-ground spectroscopic surveys which will allow us to increase significantly the number of new members in the YLA and a mean colour of the YLA members of $\langle (V - I) \rangle = 0.5$, needed to compute the Gaia end-of-mission errors.

	N	$\langle V \rangle$	Astrometric accuracy	σ_{RV} (km s^{-1})
Before Gaia	20	9	Hipparcos	4
DR1 TGAS-Hip	20	9	DR1-Hipp	2
DR1 TGAS-Tyc	50	11	DR1-Tycho	2
Gaia+	100	13	end-of-mission	0.5

TABLE I: Different scenarios for the available astrometric and spectroscopic data of a given YLA.

D. Results

The results are shown in Table II and Fig. 1. Table II uses the *DR1 TGAS-Tyc* scenario and it allows to see the effect of each of the steps of the integration process in the mean position and velocity and their dispersions. We

provide the results for each of the three Galactic models used. We note that the mean position of the association at present is not in all cases the one we imposed in the initial conditions. There may be differences of the order of $10 - 20$ pc. This fact is due to the small number of members in this association, this difference in the mean decreases when the number of members increases. The results are summarized below:

- Even though the association has the *At birth* position at about 1 kpc from the Sun, the method recovers the initial positions with an accuracy of ± 20 pc, even if we only have 50 members.
- The contribution of the positional errors in the dispersion is minimal. The dispersion observed *At present* corresponds to the initial dispersion imposed in velocities and its influences last until the *Back in time* step.
- Although the dispersion in velocities is isotropic *At birth*, the radial dispersion in positions is always larger than the tangential *Back in time*. This is probably due to the larger errors in RV which affect more the radial component. The vertical dispersion in positions is always smaller but we have to take into account that $\sigma_{\zeta'}$ depends on the age of the association because of the vertical harmonic oscillation of the system.
- The mean velocities are well recovered in all models with ± 0.5 km s^{-1} in all directions. The velocity dispersion always increases in all directions. This is evident because we convolve the intrinsic dispersion with the errors.

Fig. 1 shows the differences between the last row (*Back in time*) and the first row (*At birth*) of the previous table for each of the Galactic models and data scenarios. The results are summarized below:

- The similar results in *DR1 TGAS-Hip* and *DR1 TGAS-Tyc* can be explained in terms of a balance between the higher accuracy in *DR1 TGAS-Hip* with the larger number of members in *DR1 TGAS-Tyc*. As expected, the differences when having Gaia data and good RV are smaller with respect to previous scenarios and always less than 5 pc.
- In all cases the association is born with no dispersions in position. We only recover the positional dispersions with less than 10 pc in the *Gaia+* scenario. Therefore, the dynamical ages shall wait until the end-of-mission.
- With DR1 data (either *DR1 TGAS-Hip* or *DR1 TGAS-Tyc*) we can recover both the components of the LSR velocity and its velocity dispersion with an accuracy of less than 1 km s^{-1}. Remember that the simulated association is born with 2 km s^{-1} velocity dispersion.
- With *Gaia+* the kinematic signatures due to the potential can be checked. Already with *DR1 TGAS-Tyc* data we can interpret the dispersion ratios in terms of the potential.

III. INDICATORS OF YOUTH

From previous sections it is clear that in order to study the origin of the YLAs and membership it is essential to have available extremely accurate astrometric, photometric and spectroscopic data. Gaia and future on ground spectroscopic data will provide this information. However, it is crucial to identify the young population among this huge amount of data. Here we have studied several indicators of youth for both low and high mass stars. For low mass stars, the indicators are:

1. Rotation rates. There are semi-empirical rotational evolution models that describe a relation between rotation period and age. This models begin with an initial rotation period for young stars and then include the effects of torques and moment of inertia. Fig. 2 in [8] and Fig. 1 in [10] show the age dependence of the rotation. There is a maximum rotation for ages between 10-100 Myr which corresponds to the estimated age of the YLAs.
2. Magnetic activity is considered an age indicator because of its close connection with rotation. This connection is due to the interior dynamo that amplifies the magnetic field. Magnetic activity is due to the interaction of rotation and convection in the outer layers. Magnetic activity indices are easier to measure than rotation periods and are often assessed with a single epoch of observation. The most easily measured tracers are coronal X-ray emission, UV chromospheric and transition region emission, Ca II H K chromospheric emission, Cromospheric emission in IR Ca triplet and Hα Balmer line.
3. A phenomenological property of young stars with stellar masses <1 M$\odot$ is that Lithium is depleted during pre-main sequence (PMS) evolution. LiEW can be used as an age indicator[12].

Other indicators are, for example, the T Tauri phase of Pre-Main Sequence (PMS) low mass stars. Stars classified as T Tauri are assumed to be young. Protoplanetary disks are the outcome of the star formation process and they emit in Mid-infrared.

For massive stars the strategy is different. For stars with accurate positions in the HR diagram we can derive their ages interpolating stellar evolution models. We can achieve this accurate positions for stars with Gaia data. Apart from Gaia, there exist other surveys such as IACOB [16] and OWN [4], which contain about 600 massive OB stars with high resolution spectra that will allow also to have good positions in the HR diagram.

	Bar model						PERLAS model ($\Omega = 20$)						PERLAS model ($\Omega = 30$)					
	$\langle\xi'\rangle$	$\langle\eta'\rangle$	$\langle\zeta'\rangle$	$\langle U\rangle$	$\langle V\rangle$	$\langle W\rangle$	$\langle\xi'\rangle$	$\langle\eta'\rangle$	$\langle\zeta'\rangle$	$\langle U\rangle$	$\langle V\rangle$	$\langle W\rangle$	$\langle\xi'\rangle$	$\langle\eta'\rangle$	$\langle\zeta'\rangle$	$\langle U\rangle$	$\langle V\rangle$	$\langle W\rangle$
	$\sigma_{\xi'}$	$\sigma_{\eta'}$	$\sigma_{\zeta'}$	σ_U	σ_V	σ_W	$\sigma_{\xi'}$	$\sigma_{\eta'}$	$\sigma_{\zeta'}$	σ_U	σ_V	σ_W	$\sigma_{\xi'}$	$\sigma_{\eta'}$	$\sigma_{\zeta'}$	σ_U	σ_V	σ_W
At birth	-593.	781.	26.	-8.5	-14.	-1.9	-948.	482.	26.	-5.1	-0.3	1.5	-1269.	200.	16.	-21.7	12.7	2.5
(-50 Myr)	0	0	0	2.1	2.1	2.2	0	0	0	2.4	1.9	2.1	0	0	0	1.8	2.1	1.7
At present	-1.4	-62.2	20.5	1.3	-12.1	2.4	-26.5	-45	21	1.21	-11.6	2.3	-20.	-53.	20.	1.5	-11.9	1.9
	122.	105.	23.	3.	1.5	0.1	60.	96.	5.	2.8	0.9	2.1	33.	75.	2.	1.9	0.2	1.6
Errors	0.5	-63.7	20.7	1.3	-11.7	2.6	-25.	-46.	21.	1.23	-12.1	2.5	-20.	-53.	20.	1.85	-11.5	1.8
	124.	109.	23.	3.2	2.9	1.3	56.	89.	5.	3.4	1.7	2.1	33.	78.	2.	2.3	1.9	1.6
Back in time	-572.	781.	27.	-8.3	-13.5	-1.9	-968.	478.	26.	-5.5	-0.9	1.8	-1256.	204.	16.	-22.2	12.6	2.4
(-50 Myr)	117.	98.	13.	2.8	3.7	2.2	91.	50	2.	2.5	2.9	2.1	67.	36.	2.	2.2	2.9	1.7

TABLE II: Effects of the Data scenario *DR1 TGAS-Tyc* and the three Galactic potentials on the YLA 6D phase space evolution. Left set of values for the bar model, middle and right for the PERLAS-20 model and PERLAS-30, respectively. Mean positions and their dispersions are given in pc, while mean velocities and their dispersions are given in km s^{-1}.

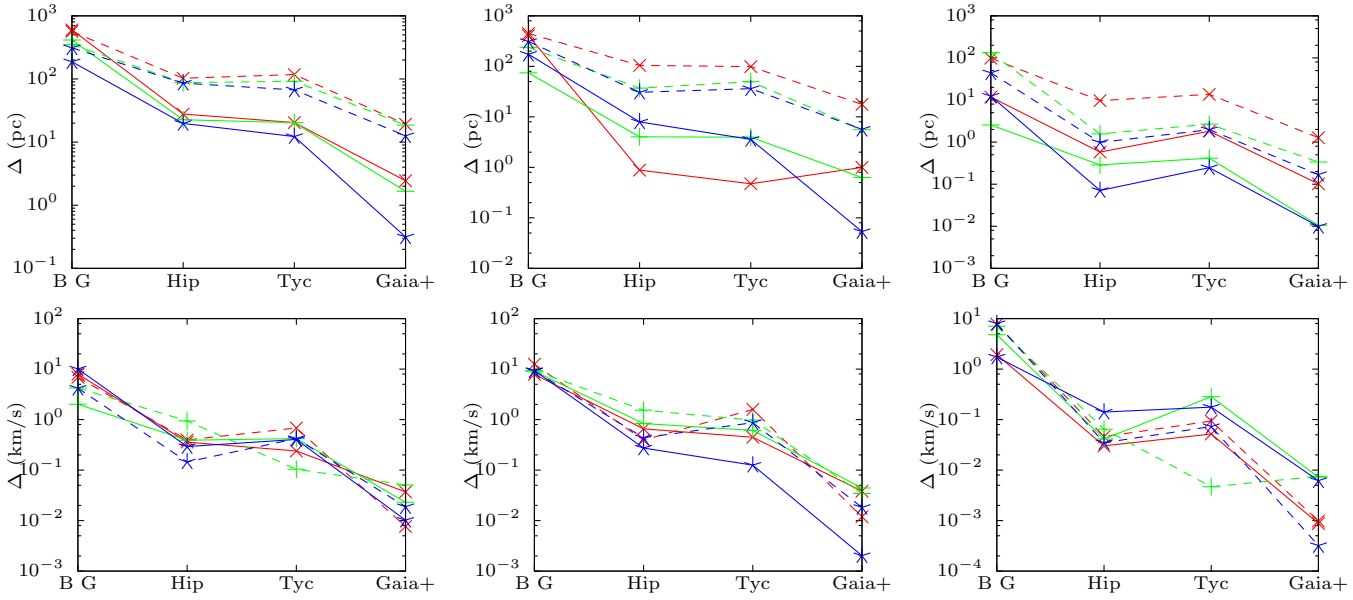

FIG. 1: Effect of the different Data scenarios on the recovery of the initial YLA mean positions and velocities (solid lines, top and bottom, respect.) and position and velocity dispersions (dashed lines, top and bottom, respect.) on the radial (ξ', U_{LSR}) (left), tangential (η', V_{LSR}) (middle) and vertical (ζ', W_{LSR}) (right) coordinates for the different Galactic models (the *Bar* model (red), the *PERLAS-20* model (green) and the *PERLAS-30* model (blue)). Note that the vertical axis is in logarithmic scale and BG stands for *Before Gaia*, Hip for *DR1 TGAS-Hip* and Tyc for *DR1 TGAS-Tyc*.

IV. GENERATING YOUNG OBJECT SAMPLES

Catalogues Tycho-2 +	Number of sources	B-V	SACY (LiEW,RV)
1RXS	6.407	4.610 (72%)	1664 (36%)
3XMM	7.145	3.469 (49%)	82 (2%)
RAVE	287.315	217.491 (76%)	481 (0.2%)

TABLE III: Results of the cross-match.

We want to generate a sample of young objects, candidates to belong to the YLAs. In order to obtain a TGAS sample with young object candidates, we will have to consider catalogues which give information on the indicators of youth listed in the previous section. Here we start by doing a first study with the current available data. Instead of TGAS we consider the Tycho-2 Catalogue [9], which contains positions and proper motions as well as two-colour photometric data for the 2.5 million brightest stars in the sky.

The main catalogues considered to obtain a sample of young objects according with the criterion listed in

section III are the following: the ROSAT All-Sky Survey Bright Star Source Catalogue (1RXS) [22] and the 3XMM Catalogue [21] contain X-ray emission, the Radial Velocity Experiment (RAVE) contains RVs and information of the IR Ca triplet, and the SACY ([17], [18]) and Binks et al. [5] contain LiEW, HαEW and RV. There are other catalogues that contain useful information but have not been used in the present work such as SuperWASP, the The Wide-field Infrared Survey Explorer (WISE), the Galaxy Evolution Explorer (GALEX) and Gaia's Radial Velocity Spectrometer (RVS).

Table III summarizes the cross-match process performed in this work. As mentioned above, we start with the Tycho-2 catalogue and we cross-match it with other X-ray surveys (ROSAT and 3XMM) or RV surveys (RAVE). The cross-matches have been performed with TOPCAT using the all-match option (one or more possible counterparts have been selected for each initial source) and with a maximum separation depending on the position accuracy of the catalogue. Only stars with $B_T - V_T \gtrsim 0.6$ have been considered due to the lithium depletion behaviour. This cut-off is equivalent to the one applied by Torres et al. [17] which is in agreement with Figure 1 from [12]. This figure shows that for stars later than K0, LiEW allows to distinguish between young and old objects. We also exclude hot objects because of the difficulty to obtain precise RVs. The number of objects in the final candidate sample is shown in the last column of Table III. Note that it is with the cross-match with ROSAT that we obtain a larger number of possible young sources. This is in part because the SACY sample also uses the same ROSAT catalogue to generate their own sample. The next step would be to run a clustering analysis, but it is out of the scope of this work.

V. CONCLUSIONS AND FUTURE WORK

In the present project we have made a viability analysis of the possibilities of studying the YLAs with the accuracies of Gaia in different data scenarios and Galactic potentials. The aim is to see whether we can determine the dynamical ages and the place of birth of these associations and the effects of the potential in the integration of their orbits. To do so, we have considered four data scenarios (*Before Gaia*, *DR1 TGAS-Hip*, *DR1 TGAS-Tyc* and *Gaia+*) and three different potential models (Bar, PERLAS-20 and PERLAS-30). We have seen that with DR1 data we are able to recover the initial positions and dispersions and thus we can study membership and the signatures of the potential. To study the dynamical ages we shall wait until Gaia end-of-mission, when the accuracies will be much better. Once we have Gaia DR1 data we will prepare samples of young objects as explained in section IV. Then, we want to apply a clustering analysis in order to see if we can recover the already known YLAs. We also expect to find more members and maybe discover new associations. At the same time, we want to integrate the orbits of the members back in time to find a possible place of birth and see if we can constrain parameters of the potential.

Acknowledgments. I would like to extend my sincere thanks to Mercè Romero and Francesca Figueras without whom this project would not have been possible.

[1] Allen, C., Santillan, A. 1991, RMXAC, 22, 255
[2] Antoja, T., Figueras, F., Romero-Gómez, M., Pichardo, B., Valenzuela, O., Moreno, E. 2011, MNRAS, 418, 1423
[3] Asiain, R., Figueras, F., Torra, J. 1999, A&A, 350, 434
[4] Barbá, R., Gamen, R., Arias, J. I., et al. 2014, RMXAC, 44, 148
[5] Binks, A. S., Jeffries, R. D., Maxted, P. F. L. 2015, MNRAS, 452, 173
[6] Gagné, J., Lafrenière, D., Doyon, R., Malo, L., Artigau, É. 2014, ApJ, 783, 121
[7] Fernández, D., Figueras, F. Torra, J. 2008, A&A, 480, 735
[8] Hartmann, L. W., Noyes, R. W. 1987, A&A, 25, 271
[9] Høg, E., Fabricius, C., Makarov, V. V., et al. 2000, A&A, 355, 27
[10] Jeffries, R. D. 2014, The Ages of Stars, EAS Publications Series, 65, 289
[11] Klutsch, A., Freire Ferrero, R., Guillout, P., Frasca, A., Marilli, E., Montes, D. 2014, A&A, 567, 30
[12] Martín, E. L. 1997, A&A, 321, 492
[13] Malo, L., Doyon, R., Lafrenière, D., Artigau, É., Gagné, J., Baron, F., Riedel, A. 2013, ApJ, 762, 88
[14] Michalik, D., Lindegren, L., Hobbs, D. 2015, A&A, 574, 115
[15] Pichardo, B., Martos, M., Moreno, E., Espresate, J. 2003, ApJ, 582, 230
[16] Simón-Díaz, S., Herrero, A. 2014, A&A, 562, 22
[17] Torres C. A. O., Quast G. R., Da Silva L., De La Reza R., Melo C. H. F., Sterzik M., 2006, A&A, 460, 695
[18] Elliott, P., Bayo, A., Melo, C. H. F., et al. 2016, A&A, 590, 28
[19] Riedel, A. R. 2016, Proceedings of the International Astronomical Union, IAU Symposium, 314, 33
[20] Romero-Gomez, M., Figueras, F., Antoja, T., Abedi, H., Aguilar, L. 2015, MNRAS, 447, 218
[21] Rosen, S. R., Webb, N. A., Watson, M. G. et al. I. 2016, A&A, 590, 22
[22] Voges, W., Aschenbach, B., Boller, T., et al. 1999, A&A, 349, 389
[23] Walter, F. M. 1986, ApJ, 306, 573
[24] van Leeuwen, F., 2007, A&A, 474, 653-664
[25] Zuckerman B., Vican L., Song I., Schneider A., 2013, ApJ, 778, 5